



# Absolute and relative estimates of genetic and environmental variance in brain structure volumes

Lachlan T. Strike<sup>1</sup> · Narelle K. Hansell<sup>1</sup> · Paul M. Thompson<sup>2</sup> · Greig I. de Zubicaray<sup>3</sup> · Katie L. McMahon<sup>4</sup> · Brendan P. Zietsch<sup>5</sup> · Margaret J. Wright<sup>1</sup>

Received: 30 October 2018 / Accepted: 30 July 2019 / Published online: 19 August 2019  
© Springer-Verlag GmbH Germany, part of Springer Nature 2019

## Abstract

Comparing estimates of the amount of genetic and environmental variance for different brain structures may elucidate differences in the genetic architecture or developmental constraints of individual brain structures. However, most studies compare estimates of relative genetic (heritability) and environmental variance in brain structure, which do not reflect differences in absolute variance between brain regions. Here we used a population sample of young adult twins and singleton siblings of twins ( $n = 791$ ;  $M = 23$  years, Queensland Twin IMaging study) to estimate the absolute genetic and environmental variance, standardised by the phenotypic mean, in the size of cortical, subcortical, and ventricular brain structures. Mean-standardised genetic variance differed widely across structures [23.5-fold range 0.52% (hippocampus) to 12.28% (lateral ventricles)], but the range of estimates within cortical, subcortical, or ventricular structures was more moderate (two to fivefold range). There was no association between mean-standardised and relative measures of genetic variance (i.e., heritability) in brain structure volumes. We found similar results in an independent sample ( $n = 1075$ ,  $M = 29$  years, Human Connectome Project). These findings open important new lines of enquiry: namely, understanding the bases of these variance patterns, and their implications regarding the genetic architecture, evolution, and development of the human brain.

**Keywords** Volume · Genetics · Magnetic resonance imaging · Twins

---

Brendan P. Zietsch and Margaret J. Wright contributed to this work equally.

**Electronic supplementary material** The online version of this article (<https://doi.org/10.1007/s00429-019-01931-8>) contains supplementary material, which is available to authorized users.

---

✉ Lachlan T. Strike  
l.strike1@uq.edu.au

<sup>1</sup> Queensland Brain Institute, University of Queensland, Brisbane, QLD 4072, Australia

<sup>2</sup> Imaging Genetics Center, University of Southern California, Los Angeles, CA 90032, USA

<sup>3</sup> Faculty of Health, Institute of Health and Biomedical Innovation, Queensland University of Technology (QUT), Brisbane, Australia

<sup>4</sup> Herston Imaging Research Facility and School of Clinical Sciences, Queensland University of Technology (QUT), Brisbane, Australia

<sup>5</sup> School of Psychology, University of Queensland, Brisbane, QLD 4072, Australia

## Introduction

Despite broad similarities (e.g., in lobar divisions, primary gyri and sulci), the anatomy of the human brain varies substantially across individuals. The majority of this variation is likely normal and has both genetic and non-genetic (i.e., environmental) causes (Gu and Kanai 2014; Jansen et al. 2015). Estimates of raw or non-standardised genetic or environmental variance in brain morphology can be compared (Kremen et al. 2012), but this is problematic, because variance may, in part, be determined by structure size, making it difficult to interpret variance differences between structures of different size. Hence, genetic and non-genetic variance components need to be standardised to facilitate comparisons across different brain regions.

Additive genetic variance is normally standardised by dividing the genetic variance by the total phenotypic variance, giving heritability ( $h^2$ ; the proportion of phenotypic variance attributed to additive genetic differences among individuals within a population). Studies show high heritability for global brain traits [e.g., intracranial volume,

0.90, or 90% (Renteria et al. 2014)], whereas estimates for specific structures across the brain vary widely (Kremen et al. 2010; Winkler et al. 2010; Schmitt et al. 2014; Renteria et al. 2014; Joshi et al. 2011). However, a problem with comparing heritability across brain regions is that higher heritability could reflect higher genetic variance, or lower environmental variance, or both; it is, therefore, uninformative with respect to patterns of actual variation across structures.

A solution is to standardise genetic and environmental variance by the phenotypic mean; then variance estimates are independent of measurement units and can be compared across traits. For additive genetic variance, this statistic equals the additive genetic variance divided by the square of the phenotypic mean (Charlesworth 1984, 1987; Hansen et al. 2011; Houle 1992) ( $I_A$ ; henceforth referred to as mean-standardised genetic variance) and provides absolute estimates of genetic variance that are robust to other sources of variance. Mean-standardised genetic variance further reflects the “evolvability” of a trait; that is, its ability to respond to natural or sexual selection (Houle 1992); see Noreikiene et al. (2015) for an application of this measure in studying models of brain evolution in stickleback fish. Here, we are interested in using mean-standardised variance estimates to empirically rank human brain structures by genetic and environmental variance, which may elucidate differences in the genetic architecture or developmental constraints of individual brain structures. This is novel when studying human brain structures, and important as it is well established that heritability estimates are generally uninformative about levels of genetic variance (Hansen et al. 2011; Houle 1992). As heritabilities have been routinely misused as measures of genetic variance, it is important to reevaluate findings, and to provide new direct estimates of genetic variation.

Only one study has examined mean-standardised genetic variance in the human brain. Miller and Penke (2007) calculated the mean-standardised genetic variance for total brain volume ( $I_A = 0.61\%$ ; based on a meta-analysis of 19 studies), and also found this estimate was substantially smaller than estimates for other human organs or life-history traits (e.g., body weight in females  $I_A = 2.46\%$ , heart ventricle volume  $I_A = 7.08\%$ ). Whether mean-standardised genetic variance for regional brain structure volumes is similarly small is unknown. Several studies comparing mean-standardised phenotypic variance in brain structure volumes provide an intriguing first look at the strength and patterns of variability in the brain. In these studies, estimates of phenotypic variance in the volume of individual brain components differed substantially across the brain (Kennedy et al. 1998; Lange et al. 1997; Allen et al. 2002) (Supplementary Table 1). These differences were found not only between structural divisions (e.g., cortical, subcortical), but also within divisions [e.g., mean-standardised phenotypic variance for

amygdala volume was substantially greater than for hippocampal volume (Lange et al. 1997)].

Here, we use a population sample of young adult twins and singleton siblings of twins from the Queensland Twin IMaging study ( $n = 791$ ) to compare, for the first time in humans, mean-standardised estimates of additive genetic, environmental, and phenotypic variance across regional brain structure volumes. In addition, we assess the association between mean-standardised and relative measures of genetic variance (i.e., heritability). We examined volumetric measures of the brain (45 cortical, subcortical, and ventricular structures), as well as total brain volume and a comparable volumetric, non-brain phenotype (body weight). To assess the generalisability of our findings, we perform the same analyses in an independent sample of twins and singletons ( $n = 1075$ ) from the Human Connectome Project.

## Method

### Participants

Participants were from the Queensland Twin IMaging (QTIM) study of brain structure and function (de Zubicaray et al. 2008; Blokland et al. 2014; Whelan et al. 2016; Chiang et al. 2011). For the present study, we included twins and singleton siblings of twins, scanned between age 15 and 30 years, for whom T1-weighted images were available. The sample consisted of 791 healthy, right-handed young adults (62% female,  $M = 23.05$  years,  $SD = 3.37$  years), including 127 monozygotic (MZ) and 162 dizygotic (DZ) twin pairs, 162 unpaired twins (i.e., usable MRI data was not available for the co-twin), and 51 siblings of twins (0–2 per family). Prior to scanning, participants were screened for neurological and psychiatric conditions, including loss of consciousness for more than 5 min, and general MRI contraindications. Zygosity of same-sex twin pairs was determined using a commercial kit (AmpFISTR Profiler Plus Amplification Kit, ABI) and later confirmed by genome-wide single nucleotide polymorphism genotyping (Illumina 610 K chip). The study was approved by the Human Research Ethics Committees at the University of Queensland, QIMR Berghofer Medical Research Institute, and UnitingCare Health. Written informed consent was obtained from all participants, including a parent or guardian for those aged under 18 years. Participants received an honorarium for their time and to cover any transport expenses.

### Image acquisition and processing

Imaging was conducted on a 4T Bruker Medspec (Bruker, Germany) whole-body MRI system paired with a transverse electromagnetic (TEM) head coil. Structural T1-weighted

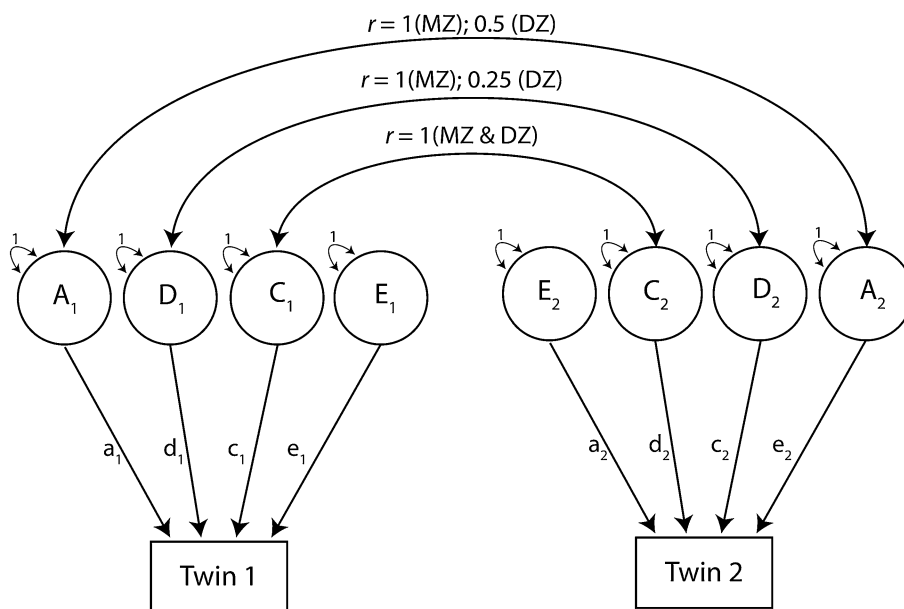
3D images were acquired (TR = 1500 ms, TE = 3.35 ms, TI = 700 ms, 230 mm FOV, 0.9 mm slice thickness, 256 slices). Scans were corrected for intensity inhomogeneity with SPM12 (Wellcome Trust Centre for Neuroimaging, London, UK; <http://www.fil.ion.ucl.ac.uk/spm>) prior to extracting cortical, subcortical, and ventricular volumes (mm<sup>3</sup>) using FreeSurfer v5.3 (<http://surfer.nmr.mgh.harvard.edu>); see Fischl (2012) for a summary of the FreeSurfer methodology. These included volumes for 34 cortical [regions of interest (ROI) from the Desikan–Killiany atlas (Desikan et al. 2006)] and 7 subcortical (hippocampus, amygdala, putamen, caudate, thalamus, nucleus accumbens, globus pallidus) structures per hemisphere, as well as the lateral ventricle and choroid plexus from each hemisphere, and the 3rd and 4th ventricles. In addition, total brain segmentation volume (FreeSurfer variable *BrainSegVol*) was extracted. Structure segmentation and labelling were checked using the procedures of the ENIGMA consortium ([enigma.ini.usc.edu](http://enigma.ini.usc.edu)), with incorrectly delineated structures excluded from the analysis (number of excluded structures listed in Supplementary Table 2). For each bilateral structure, we then computed a mean volume using the left and right hemisphere volumes. The test–retest reliability of imaging measures was estimated using intra-class correlation coefficients (ICC; two-way mixed effects, absolute agreement, single measurement) for a subset of participants scanned twice ( $n = 45$ , mean rescan interval  $113.15 \pm 56.30$  days).

**Estimation of variance components**

Saturated models were fit to the data to compare brain volume means, variances, and covariances, as well as to

estimate correlations between MZ and DZ twin pairs. Genetic and environmental variances in subcortical, cortical, and ventricular volumes were then examined using a classic twin study. Briefly, the classic twin design (Fig. 1) contrasts the observed covariance between MZ twins and DZ twins to partition the variance in a phenotype into four sources: additive genetic (A), non-additive genetic (D, e.g., dominance and epistasis), common or shared environment (C), and unique or non-shared environment (E) (Neale and Cardon 1992). Correlations between additive genetic factors (A) are fixed to 1 for MZ and 0.5 for DZ twins as MZ and DZ twins share 100% and (on average) 50% of their genetic material, respectively. For dominance genetic effects (D), correlations are fixed at 1 for MZ twins and 0.25 for DZ twins, and for common environment effects (C), correlations are fixed at 1 for both MZ and DZ twins. Unique environment effects (E) are uncorrelated between twin pairs as this represents environmental influence affecting one twin only. Estimates of unique environment also include measurement error, as it is random and unrelated to twin similarity. As C and D are confounded in a classic twin study (C effects increase twin similarity; D effects decrease twin similarity) they cannot be estimated simultaneously (i.e., either an ACE or ADE model is selected). Here, the classic twin model was modified to include non-twin siblings (maximum of two per family) to increase statistical power (Posthuma and Boomsma 2000). The maximum-likelihood structural equation modelling package *OpenMx 2.13.2* (Neale et al. 2016) in *R 3.5.3* (R Core Team 2019) was used to determine the combination of A, D, C, and E that best contribute to variance in a phenotype, and covariance between individuals for each phenotype. Akaike’s Information Criteria (AIC) (de

**Fig. 1** Classic twin design. The model partitions the variance in a phenotype into additive genetic (A), non-additive genetic (D, e.g., dominance and epistasis), common or shared environment (C) and unique or non-shared environment (E) sources. a, d, c, and e represent parameters estimates for A, D, C, and E, respectively. In the present study, the classic twin model was extended to include non-twin siblings (maximum of two per family); only two family members (twin 1 and twin 2) are shown here



Leeuw 1992) was used to compare the fit of ACE or ADE models (and also submodels containing only AE, CE, and E variance sources) to find the most parsimonious model (a smaller AIC value indicates a better model fit). Adjustments for age and sex were included in the models to remove the influence of these variables. 95% maximum-likelihood confidence intervals were estimated for all variance measures through *OpenMx*.

### Mean-standardised absolute variance

Estimates of raw/non-standardised variance for each phenotype were then standardised by the phenotypic mean. For example, mean-standardised additive genetic variance ( $I_A$ ) equals the additive genetic variance ( $V_A$ ) divided by the phenotypic mean of the trait squared:

$$I_A = \frac{V_A}{\bar{x}^2}.$$

Mean-standardised genetic variance is also commonly expressed as the coefficient of additive genetic variance ( $CV_A$ ) (Hansen et al. 2011; Houle 1992), which is intrinsically related to the measure of mean-standardised genetic variance used in the present study ( $I_A = CV_A^2$ ).  $I_A$  is favoured in studies of evolvability or artificial selection, since it is interpreted as the expected percentage change per generation under a unit of selection (Garcia-Gonzalez et al. 2012; Hansen et al. 2003, 2011). Furthermore, we scaled estimates of additional variance components (i.e., non-additive genetic, common environment, and unique environment), as well as total phenotypic variance, by the phenotypic mean to produce mean-standardised estimates for these variance amounts. Lastly, we calculated relative estimates of genetic and environmental variance by dividing raw variance estimates by total phenotypic variance. Both mean-standardised and relative variance estimates are dimensionless units, which can be expressed as a percentage. For comparison with a volumetric, non-brain phenotype, we also estimated mean-standardised variance components of body weight (kilograms).

### Correction for total brain volume

Previous studies have shown associations between total brain volume and the volumes of individual brain structures (Renteria et al. 2014; Wen et al. 2016; Eyler et al. 2011). To examine if variance in individual structure volumes is simply a reflection of variation in total brain volume, we recalculated the mean-standardised variance estimates after removing the effects of a global covariate (i.e., total brain volume; adjustments included in twin models).

### Replication in an independent sample

Data from the Human Connectome Project (HCP: S1200 release) (Van Essen et al. 2012; Glasser et al. 2016) was used as a secondary analysis sample. We excluded participants with incorrectly delineated cortical surfaces ( $n=3$ ), and participants that were third or higher order singleton siblings ( $n=5$ ) or half-siblings ( $n=30$ ). The final data set consisted of 1075 adults (583 females,  $M=28.81$  years,  $SD=3.70$  years), comprising of 152 monozygotic (MZ) and 85 dizygotic (DZ) twin pairs, 16 unpaired twins, 208 siblings of twins (0–2 per family), and 377 members of singleton families (1–4 per family). MZ and DZ twin zygosity was determined through genotyping, if available (215 of 237 pairs), otherwise by self-report (22 of 237 pairs). Details relating to participant selection and MRI acquisition have been reported elsewhere (Van Essen et al. 2012). All analyses completed on the QTIM sample were undertaken on the HCP data, including test–retest reliability on a sub-sample of participants who were scanned twice ( $n=45$ , mean duration between first and second scan was  $139.30 \pm 68.99$  days).

### Results

For most volumes (36 out of 47), the AE model (specifying additive genetic (A) and unique environment (E) variance sources only) was the best fitting model (lowest AIC value; Supplementary Table 3). The full ACE or ADE model was a slightly better fit for the remaining 11 volumes. In addition, the average of correlations between DZ pairs was very close to one-half the average of correlations between MZ pairs (Supplementary Table 2), which is the expected pattern if twin similarity arises solely due to additive genetic effects. Based on these results, and also for ease of interpretation and comparison, we present results for AE models in the main text. We note that our decision to drop D and C effects could overestimate A effects for some brain volumes, and we provide the full ACE/ADE models (where applicable) in Supplementary Table 3. The average of estimates of mean-standardised genetic variance ( $I_A$ ) in the QTIM data set were highest for ventricular structures (6.29% compared to < 1% for cortical and subcortical structure volumes), and considerably higher than for body weight (2.85%) (Table 1, Supplementary Fig. 1). Furthermore, mean-standardised genetic variance for cortical and subcortical structures (0.98% and 0.77%, respectively) was, on average, higher than for total brain volume ( $I_A=0.44\%$ ).

Table 1 and Figs. 2a, 3a, d show estimates of  $I_A$  ranged from a low of 0.52% for the hippocampus to a high of 12.28% for the lateral ventricles, representing a 23.5-fold range in mean-standardised genetic variance across the brain structure volumes examined. However, this wide

**Table 1** Phenotypic mean, mean-standardised genetic ( $I_A$ ), environmental ( $I_E$ ), phenotypic ( $I_P$ ), and relative genetic ( $h^2$ ) variance estimates for cortical, subcortical, and ventricular volumes, as well as total brain volume and body weight, in the QTIM and HCP data sets

	QTIM				HCP					
	Mean	$I_A$ (95% CI)	$I_E$ (95% CI)	$I_P$ (95% CI)	$h^2$	Mean	$I_A$ (95% CI)	$I_E$ (95% CI)	$I_P$ (95% CI)	$h^2$
<b>Cortical</b>										
<b>Frontal</b>										
Superior frontal	24,142	0.60 (0.53, 0.69)	0.15 (0.12, 0.19)	0.75 (0.68, 0.83)	0.80	24,210	0.86 (0.77, 0.95)	0.12 (0.09, 0.14)	0.97 (0.89, 1.07)	0.88
Rostral middle frontal	16,616	0.94 (0.81, 1.10)	0.35 (0.28, 0.46)	1.30 (1.18, 1.45)	0.73	17,955	1.01 (0.90, 1.14)	0.20 (0.16, 0.25)	1.21 (1.11, 1.32)	0.84
Caudal middle frontal	6791	1.54 (1.26, 1.84)	0.71 (0.59, 0.90)	2.25 (2.03, 2.49)	0.68	6971	1.53 (1.33, 1.78)	0.75 (0.63, 0.88)	2.28 (2.10, 2.50)	0.67
Pars opercularis	4972	0.93 (0.73, 1.11)	0.65 (0.53, 0.77)	1.58 (1.43, 1.76)	0.59	5062	1.25 (1.04, 1.44)	0.65 (0.53, 0.79)	1.90 (1.75, 2.09)	0.66
Pars triangularis	4276	0.73 (0.47, 1.00)	1.03 (0.83, 1.21)	1.77 (1.60, 1.96)	0.41	4340	1.08 (0.92, 1.31)	0.79 (0.66, 0.96)	1.88 (1.72, 2.06)	0.58
Pars orbitalis	2444	0.65 (0.45, 0.87)	0.80 (0.65, 0.94)	1.46 (1.32, 1.62)	0.45	2579	0.83 (0.69, 0.95)	0.39 (0.33, 0.45)	1.21 (1.10, 1.33)	0.68
Lateral orbitofrontal	6980	0.80 (0.65, 0.94)	0.40 (0.32, 0.50)	1.20 (1.08, 1.34)	0.67	8241	0.77 (0.68, 0.87)	0.18 (0.15, 0.22)	0.95 (0.87, 1.04)	0.82
Medial orbitofrontal	4982	0.66 (0.48, 0.80)	0.65 (0.55, 0.81)	1.31 (1.18, 1.45)	0.50	5812	0.71 (0.60, 0.81)	0.29 (0.24, 0.36)	1.00 (0.92, 1.09)	0.71
Precentral	14,219	0.69 (0.60, 0.79)	0.19 (0.15, 0.24)	0.88 (0.80, 0.98)	0.78	14,706	0.77 (0.68, 0.86)	0.14 (0.11, 0.17)	0.91 (0.83, 0.99)	0.85
Paracentral	3950	1.07 (0.87, 1.29)	0.56 (0.44, 0.70)	1.63 (1.46, 1.81)	0.66	4070	1.25 (1.10, 1.41)	0.42 (0.34, 0.52)	1.67 (1.54, 1.83)	0.75
Frontal pole	994	0.92 (0.56, 1.29)	1.66 (1.45, 2.04)	2.58 (2.34, 2.86)	0.36	950	0.82 (0.58, 1.07)	1.13 (0.94, 1.35)	1.95 (1.79, 2.13)	0.42
<b>Parietal</b>										
Superior parietal	14,133	0.82 (0.71, 0.94)	0.25 (0.20, 0.31)	1.07 (0.97, 1.19)	0.76	14,027	0.99 (0.88, 1.10)	0.20 (0.16, 0.25)	1.19 (1.09, 1.29)	0.83
Inferior parietal	14,650	0.81 (0.67, 0.96)	0.37 (0.30, 0.45)	1.18 (1.06, 1.32)	0.68	15,160	0.93 (0.82, 1.06)	0.35 (0.29, 0.42)	1.29 (1.18, 1.41)	0.72
Supramarginal	11,548	0.86 (0.74, 1.01)	0.35 (0.27, 0.44)	1.20 (1.09, 1.34)	0.71	11,591	0.98 (0.86, 1.15)	0.42 (0.35, 0.51)	1.40 (1.29, 1.53)	0.7
Postcentral	9952	0.82 (0.70, 0.98)	0.39 (0.31, 0.49)	1.21 (1.09, 1.35)	0.68	10,397	0.83 (0.70, 0.97)	0.34 (0.29, 0.42)	1.18 (1.07, 1.29)	0.71
Precuneus	10,729	0.81 (0.71, 0.95)	0.23 (0.19, 0.30)	1.05 (0.95, 1.16)	0.78	11,109	0.93 (0.83, 1.05)	0.20 (0.17, 0.25)	1.14 (1.05, 1.24)	0.82
<b>Occipital</b>										
Lateral occipital	12,048	0.71 (0.58, 0.82)	0.31 (0.25, 0.39)	1.02 (0.91, 1.13)	0.70	12,196	1.11 (0.98, 1.26)	0.31 (0.25, 0.38)	1.41 (1.29, 1.54)	0.78
Lingual	7008	0.98 (0.82, 1.16)	0.36 (0.28, 0.45)	1.34 (1.20, 1.48)	0.73	7590	1.36 (1.22, 1.54)	0.31 (0.25, 0.38)	1.67 (1.52, 1.82)	0.82
Cuneus	3216	1.23 (1.01, 1.43)	0.52 (0.41, 0.66)	1.75 (1.57, 1.94)	0.70	3540	1.30 (1.13, 1.48)	0.43 (0.36, 0.53)	1.74 (1.58, 1.89)	0.75
Pericalcarine	2362	2.01 (1.77, 2.30)	0.36 (0.29, 0.47)	2.37 (2.15, 2.65)	0.85	2994	2.09 (1.86, 2.33)	0.34 (0.28, 0.42)	2.42 (2.23, 2.66)	0.86
<b>Temporal</b>										
Superior temporal	11,831	0.61 (0.49, 0.73)	0.38 (0.30, 0.48)	0.99 (0.90, 1.11)	0.62	12,845	0.84 (0.75, 0.95)	0.23 (0.18, 0.28)	1.06 (0.97, 1.16)	0.79
Middle temporal	9948	0.85 (0.66, 1.05)	0.69 (0.57, 0.86)	1.54 (1.39, 1.72)	0.55	12,421	0.97 (0.87, 1.11)	0.25 (0.21, 0.31)	1.23 (1.13, 1.35)	0.79
Inferior temporal	8586	1.26 (1.02, 1.52)	0.74 (0.60, 0.93)	2.00 (1.81, 2.23)	0.63	11,718	1.27 (1.12, 1.44)	0.43 (0.35, 0.51)	1.70 (1.55, 1.87)	0.75
Banks superior temporal sulcus	2549	0.96 (0.68, 1.25)	0.98 (0.78, 1.24)	1.94 (1.75, 2.16)	0.49	2788	1.09 (0.87, 1.32)	0.71 (0.58, 0.87)	1.79 (1.64, 1.97)	0.61
Fusiform	9154	0.83 (0.66, 1.00)	0.47 (0.37, 0.59)	1.30 (1.17, 1.44)	0.64	11,065	0.95 (0.83, 1.08)	0.38 (0.32, 0.46)	1.33 (1.22, 1.45)	0.71
Transverse temporal	1095	1.36 (1.07, 1.69)	1.09 (0.88, 1.29)	2.45 (2.21, 2.73)	0.56	1247	1.56 (1.36, 1.79)	0.81 (0.70, 0.97)	2.38 (2.19, 2.61)	0.66
Entorhinal	1386	1.42 (0.98, 1.87)	1.77 (1.44, 2.19)	3.19 (2.89, 3.53)	0.44	1739	1.63 (1.32, 1.96)	1.15 (0.96, 1.39)	2.78 (2.54, 3.06)	0.59
Temporal pole	2018	1.44 (0.99, 1.84)	1.87 (1.52, 2.30)	3.31 (2.99, 3.67)	0.43	2328	0.58 (0.41, 0.77)	0.99 (0.88, 1.12)	1.57 (1.45, 1.72)	0.37

Table 1 (continued)

	QTIM			HCP					
	Mean	$I_A$ (95% CI)	$I_E$ (95% CI)	$I_P$ (95% CI)	Mean	$I_A$ (95% CI)	$I_E$ (95% CI)	$I_P$ (95% CI)	$h^2$
Parahippocampal Cingulate	2249	0.73 (0.57, 0.87)	0.45 (0.36, 0.55)	1.19 (1.07, 1.33)	0.62	1.18 (1.03, 1.37)	0.46 (0.37, 0.57)	1.64 (1.51, 1.80)	0.72
Rostral anterior cingulate	2607	1.27 (0.96, 1.60)	1.14 (0.97, 1.42)	2.42 (2.18, 2.69)	0.53	1.68 (1.37, 1.94)	0.85 (0.68, 1.07)	2.53 (2.30, 2.79)	0.66
Caudal anterior cingulate	2151	1.15 (0.77, 1.54)	1.59 (1.37, 1.95)	2.73 (2.47, 3.04)	0.42	1.69 (1.25, 2.15)	1.34 (1.06, 1.69)	3.03 (2.76, 3.35)	0.56
Posterior cingulate	3455	0.78 (0.61, 0.97)	0.64 (0.54, 0.79)	1.42 (1.29, 1.58)	0.55	1.06 (0.92, 1.25)	0.49 (0.40, 0.61)	1.55 (1.42, 1.71)	0.68
Isthmus cingulate	2698	1.28 (1.09, 1.54)	0.64 (0.53, 0.81)	1.92 (1.73, 2.14)	0.67	1.29 (1.07, 1.49)	0.65 (0.55, 0.80)	1.94 (1.76, 2.13)	0.67
Insular									
Insular	6806	0.66 (0.54, 0.78)	0.29 (0.24, 0.37)	0.95 (0.85, 1.05)	0.69	0.66 (0.58, 0.75)	0.24 (0.20, 0.28)	0.89 (0.82, 0.97)	0.73
Subcortical									
Thalamus	7718	0.55 (0.47, 0.62)	0.10 (0.08, 0.13)	0.65 (0.59, 0.72)	0.84	0.62 (0.54, 0.70)	0.17 (0.14, 0.21)	0.79 (0.72, 0.86)	0.79
Putamen	6067	0.73 (0.65, 0.83)	0.09 (0.07, 0.11)	0.82 (0.74, 0.91)	0.89	0.85 (0.76, 0.95)	0.17 (0.14, 0.21)	1.02 (0.93, 1.12)	0.83
Hippocampus	4160	0.52 (0.46, 0.60)	0.11 (0.09, 0.14)	0.63 (0.57, 0.70)	0.83	0.66 (0.59, 0.73)	0.08 (0.07, 0.10)	0.74 (0.68, 0.81)	0.89
Caudate	4050	1.02 (0.90, 1.15)	0.12 (0.09, 0.15)	1.13 (1.02, 1.25)	0.90	1.07 (0.96, 1.19)	0.18 (0.15, 0.23)	1.25 (1.15, 1.38)	0.85
Amygdala	1673	0.77 (0.63, 0.91)	0.38 (0.30, 0.49)	1.16 (1.04, 1.29)	0.67	0.87 (0.76, 0.98)	0.17 (0.14, 0.21)	1.03 (0.95, 1.13)	0.84
Globus pallidus	1581	0.55 (0.44, 0.66)	0.26 (0.21, 0.34)	0.81 (0.74, 0.90)	0.67	1.12 (0.94, 1.31)	0.51 (0.42, 0.61)	1.63 (1.49, 1.78)	0.69
Nucleus accumbens	708	1.24 (1.05, 1.50)	0.71 (0.57, 0.89)	1.95 (1.77, 2.17)	0.64	1.42 (1.26, 1.63)	0.44 (0.36, 0.55)	1.86 (1.72, 2.05)	0.76
Ventricular									
Lateral ventricle	6281	12.28 (9.66, 15.00)	6.78 (5.33, 8.71)	19.06 (17.15, 21.28)	0.64	17.58 (15.24, 20.87)	8.89 (7.20, 11.01)	26.46 (24.13, 29.13)	0.66
3rd ventricle	739	3.77 (3.05, 4.54)	1.84 (1.51, 2.34)	5.61 (5.09, 6.26)	0.67	7.64 (6.82, 8.69)	1.54 (1.22, 1.99)	9.18 (8.45, 10.13)	0.83
4th ventricle	1640	6.44 (5.45, 7.52)	2.24 (1.80, 2.83)	8.68 (7.88, 9.68)	0.74	8.94 (8.01, 9.99)	1.67 (1.36, 2.09)	10.61 (9.76, 11.67)	0.84
Choroid plexus	1257	2.65 (2.30, 3.06)	0.95 (0.77, 1.16)	3.60 (3.27, 4.01)	0.74	2.63 (2.24, 2.99)	0.89 (0.72, 1.12)	3.53 (3.21, 3.88)	0.75
Global									
Total brain volume	1,137,297	0.44 (0.42, 0.66)	0.04 (0.02, 0.06)	0.48 (0.47, 0.72)	0.91	1,182,050	0.71 (0.48, 0.92)	0.06 (0.03, 0.07)	0.78 (0.59, 0.80)
Body weight	69	2.85 (2.42, 3.34)	0.90 (0.72, 1.15)	3.76 (3.37, 4.21)	0.76	78	3.36 (2.88, 3.80)	0.98 (0.79, 1.24)	4.34 (3.95, 4.78)

All estimates are taken from AE models (corrected for age and sex). Raw variance components can be calculated by multiplying the mean-standardised variance estimate by the square of the phenotypic mean. Relative environmental variance is calculated as  $1 - h^2$ .

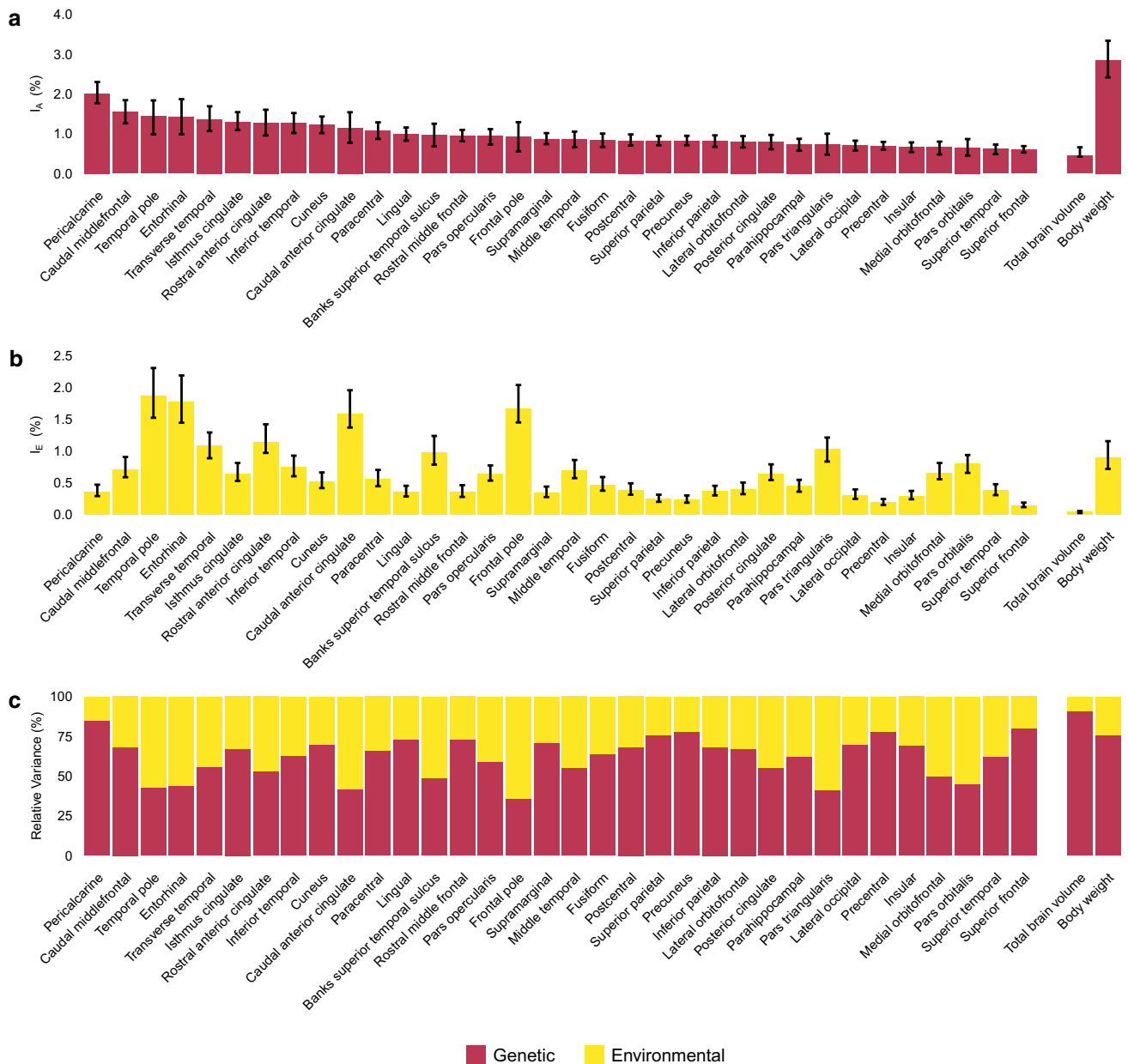


**Fig. 2** Absolute (mean-standardised) genetic (a) and environmental (b) variances (with 95% confidence intervals), as well as relative genetic and environmental variance components (c) for cortical structures in the QTIM data set. Estimates are presented in descending order of genetic variance. Mean-standardised genetic variance was largest for the pericalcarine cortex, and smallest for the superior frontal gyrus (a). Many structures had greater mean-standardised genetic variance than total brain volume (21/34 structures with non-overlapping confidence intervals with total brain volume), and all corti-

cal structures had less mean-standardised genetic variance than body weight. For the majority of structures, mean-standardised genetic variance estimates were greater than corresponding environmental variance estimates, though 95% confidence intervals overlapped for a number of structures (b). Moderate relative genetic variance ( $h^2 \sim 50\%$ ) was due to low mean-standardised genetic variance (e.g., pars triangularis, pars orbitalis, medial orbitofrontal) or high mean-standardised environmental variance (e.g., temporal pole, entorhinal, frontal pole)

range in  $I_A$  was substantially reduced when the ventricular structures were excluded ( $I_A$  0.52–2.01%, fourfold range), and within each of the structural divisions we observed a similarly reduced range in  $I_A$ : cortical 3.4-fold (Fig. 2a), subcortical 2.4-fold (Fig. 3a), ventricular 4.6-fold (Fig. 3d).

For the majority of structures, mean-standardised genetic variance estimates were greater than corresponding environmental variance estimates, though 95% confidence intervals overlapped for a number of structures (Figs. 2b, 3b, e; Table 1). An exception to this was the frontal pole, where the

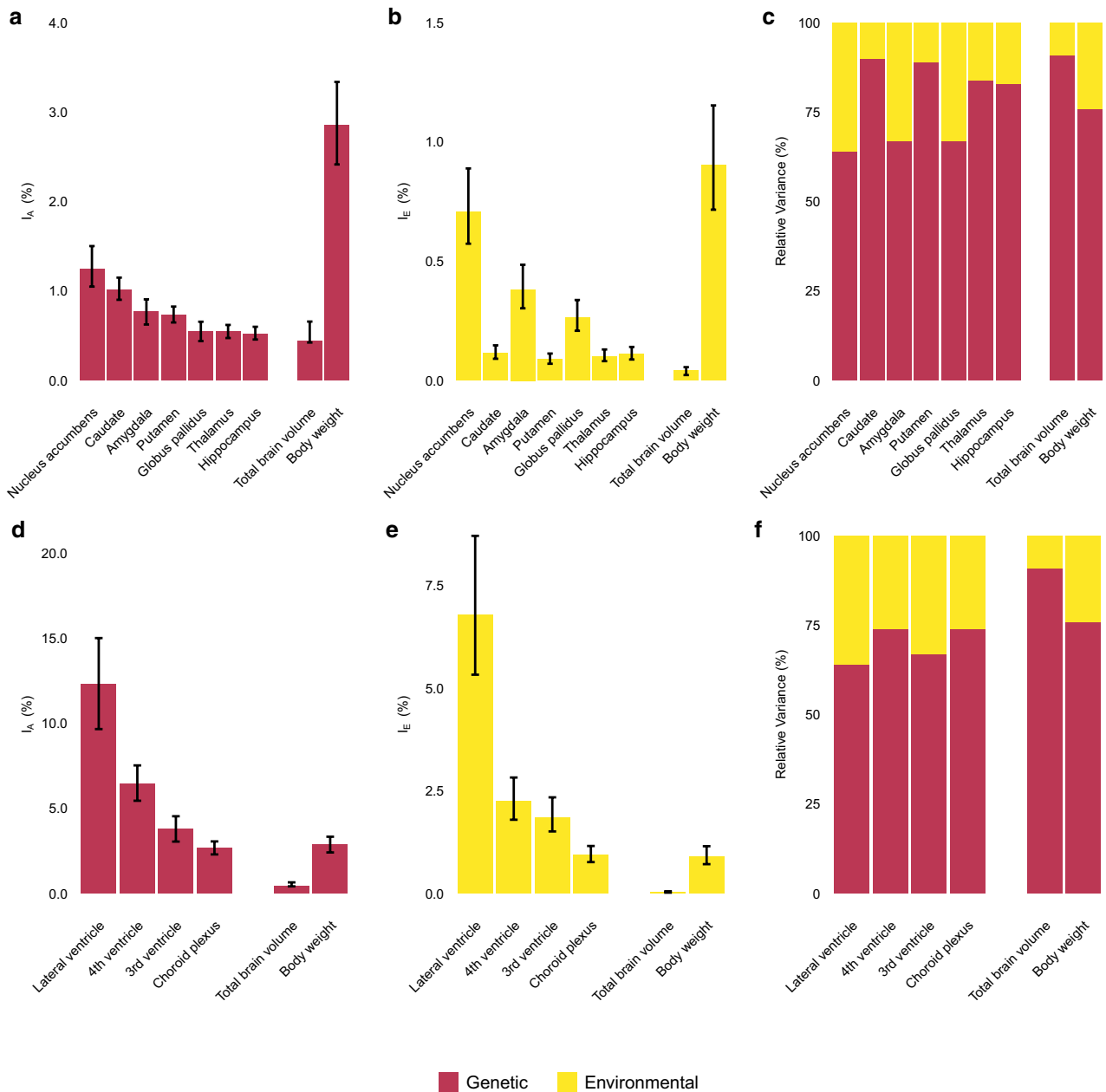


**Fig. 3** Absolute (mean-standardised) genetic (a, d) and environmental (b, e) variances (with 95% confidence intervals), as well as relative genetic and environmental variance components (c, f) for subcortical (top row) and ventricular (bottom row) structures in the QTIM data set. Estimates are presented in descending order of mean-standardised genetic variance. For subcortical structures, mean-standardised genetic variance was largest for the nucleus accumbens, and smallest for the hippocampus (a). Mean-standardised genetic variance estimates for the amygdala, putamen, globus pallidus, thalamus, and hippocampus overlapped with the estimate for total brain volume. For

ventricular structures, genetic and environmental variance was largest for the lateral ventricles, and smallest for the choroid plexus (d, e). Mean-standardised environmental variance was smaller than corresponding genetic variance for all subcortical (b) and ventricular structures (e). Despite having the highest mean-standardised genetic variance for their structure type, the nucleus accumbens (subcortical) and lateral ventricles (ventricular) had more moderate relative genetic variance (c, f) on account of the large environmental variance for these structures

mean-standardised environmental variance estimate (which includes measurement error) was significantly greater than the corresponding genetic estimate [ $I_A \pm 95\% \text{ CI } 0.92\% (0.56, 1.29)$ ,  $I_E \pm 95\% \text{ CI } 1.66\% (1.45, 2.04)$ ]. Structures

with low mean-standardised genetic variance ( $I_A < 0.75\%$ ) had high test–retest estimates ( $\text{ICC} > 0.80$ ; Supplementary Table 2), suggesting that the low  $I_A$  estimates were not a result of large measurement error.

There was 2.5-fold range in relative genetic variance estimates (i.e., heritability) across brain structures (frontal pole  $h^2$  36% to caudate  $h^2$  90%; Figs. 2c, 3c, d; Table 1); a substantially smaller range compared to the 23.5-fold range in mean-standardised genetic variance. The correlation between mean-standardised and relative genetic variance estimates for brain structures was not significant (Fig. 4). Cortical and subcortical structures with high relative genetic variance ( $h^2 > 75\%$ ) generally had more moderate mean-standardised variance ( $I_A$  range 0.55–1.02%), with high mean-standardised and relative genetic variance found only for the pericalcarine cortex ( $I_A = 2.01\%$ ,  $h^2 = 85\%$ ). Moderate relative genetic variance ( $h^2 \sim 50\%$ ) was due to low mean-standardised genetic variance (e.g., pars triangularis, pars orbitalis, medial orbitofrontal) or high mean-standardised environmental variance (e.g., temporal pole, entorhinal, frontal pole). Relative genetic variance estimates for ventricular structures, which had significantly higher mean-standardised genetic variance ( $I_A$  range 2.65–12.28%) than cortical/subcortical structures [ $I_A$  range 0.52–2.01%], ranged from 64 to 74%.

When we repeated the analysis with a global covariate (total brain volume), all brain volumes had smaller mean-standardised genetic variance estimates (Supplementary Table 4). The average fold change between  $I_A$  estimates without and with adjustment for a global covariate was  $-1.76$  for cortical,  $-1.46$  for subcortical, and  $-1.07$  for ventricular volumes. Mean-standardised phenotypic variance estimates were reduced to a similar extent for all structures following adjustment for total brain volume (average fold change

$-1.43$  for cortical,  $-1.36$  for subcortical, and  $-1.05$  for ventricular volumes), and mean-standardised environmental variance estimates changed only slightly (average fold change  $-1.08$  for cortical,  $-1.11$  for subcortical, and  $-1.02$  for ventricular volumes). However, there was still significant variance remaining for all volumes after correcting for total brain volume, indicating that structures' variance was not simply total brain size variance. Furthermore, patterns of mean-standardised variance (after adjustment for a global covariate; Supplementary Figs. 2 and 3) were broadly consistently with patterns of variance without adjustment for a global covariate (Figs. 2, 3).

### Replication using the HCP sample

Similar to the QTIM data set, estimates from AE models (AE model best fitting for 33/47 volumes) are presented in text, with estimates from ACE/ADE models presented in Supplementary 5. Estimates of mean-standardised genetic variance were, on average, similar in the HCP data set compared to the QTIM data set (Table 1, Supplementary Fig. 1). The lateral ventricles had the largest mean-standardised genetic variance in the HCP data set, and this estimate was substantially larger than in the QTIM data set [ $I_A \pm 95\%$  CI HCP 17.58% (15.24, 20.87), QTIM 12.28% (9.66, 15.00)]. Estimates of mean-standardised genetic variance for cortical structures followed a similar pattern for both data sets (Fig. 5), but some differences were present [e.g., temporal pole  $I_A \pm 95\%$  CI HCP 0.58% (0.41, 0.77), QTIM 1.44% (0.99, 1.84)]. In both samples, mean-standardised genetic

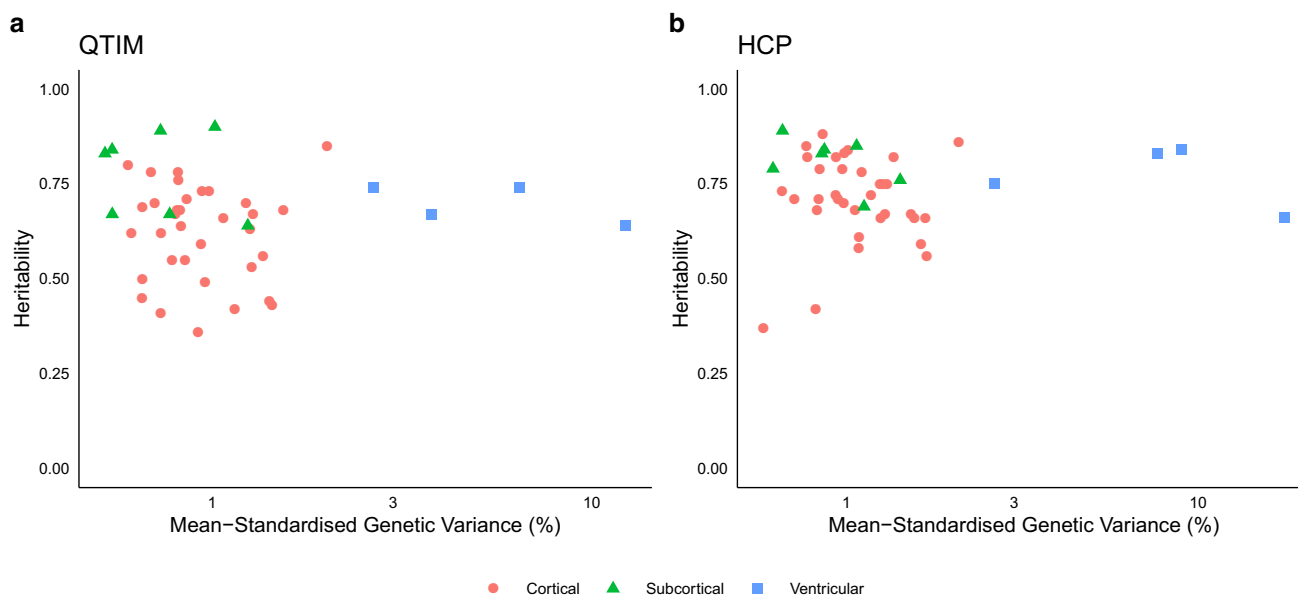


**Fig. 4** Plot of absolute (mean-standardised;  $I_A$ ) and relative (heritability;  $h^2$ ) genetic variance estimates in the QTIM (a) and HCP (b) data sets, separated by structure type. Note that the x-axis is presented on

a log<sub>10</sub> scale. The correlation between  $I_A$  and  $h^2$  was 0.03 and 0.02 in the QTIM and HCP data sets, respectively (both correlations were not significant)

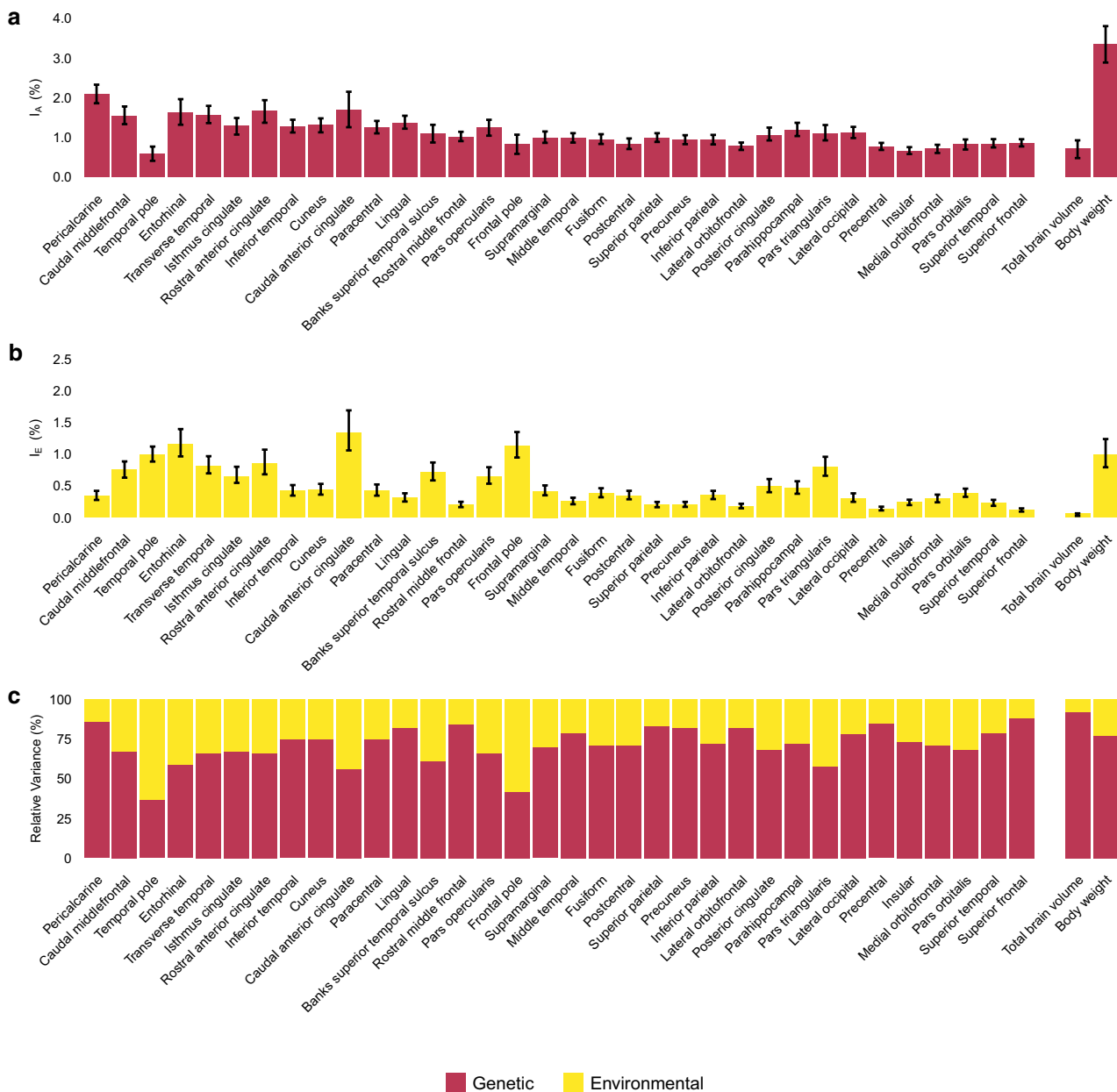


**Fig. 5** Absolute (mean-standardised) genetic (a) and environmental (b) variances (with 95% confidence intervals), as well as relative genetic and environmental variance components (c) for cortical struc-

tures in the HCP data set. Estimates are presented in descending order of mean-standardised genetic variance in the QTIM data set (Fig. 2)

variance in subcortical structures was largest for the nucleus accumbens, with smaller estimates for the hippocampus and thalamus (Fig. 6). Similar to QTIM, low mean-standardised genetic variance estimates were unlikely to be the result of large measurement unreliability (Supplementary Table 2), and the correlation between mean-standardised and relative genetic variance estimates (i.e., heritability) was not significant (Fig. 4). In addition, the effect of correcting for total brain volume was similar to that in the QTIM data set (Supplementary Table 5, Supplementary Figs. 4 and 5).

### Discussion

Here, for the first time in humans, we examine the mean-standardised genetic and environmental variance in the size of cortical, subcortical, and ventricular brain structure volumes. In contrast to relative estimates (e.g., heritability), which have been widely used in imaging genetics studies, the mean-standardised approach does not scale raw variance components to total phenotypic variance. Instead, it estimates the absolute genetic and environmental variance

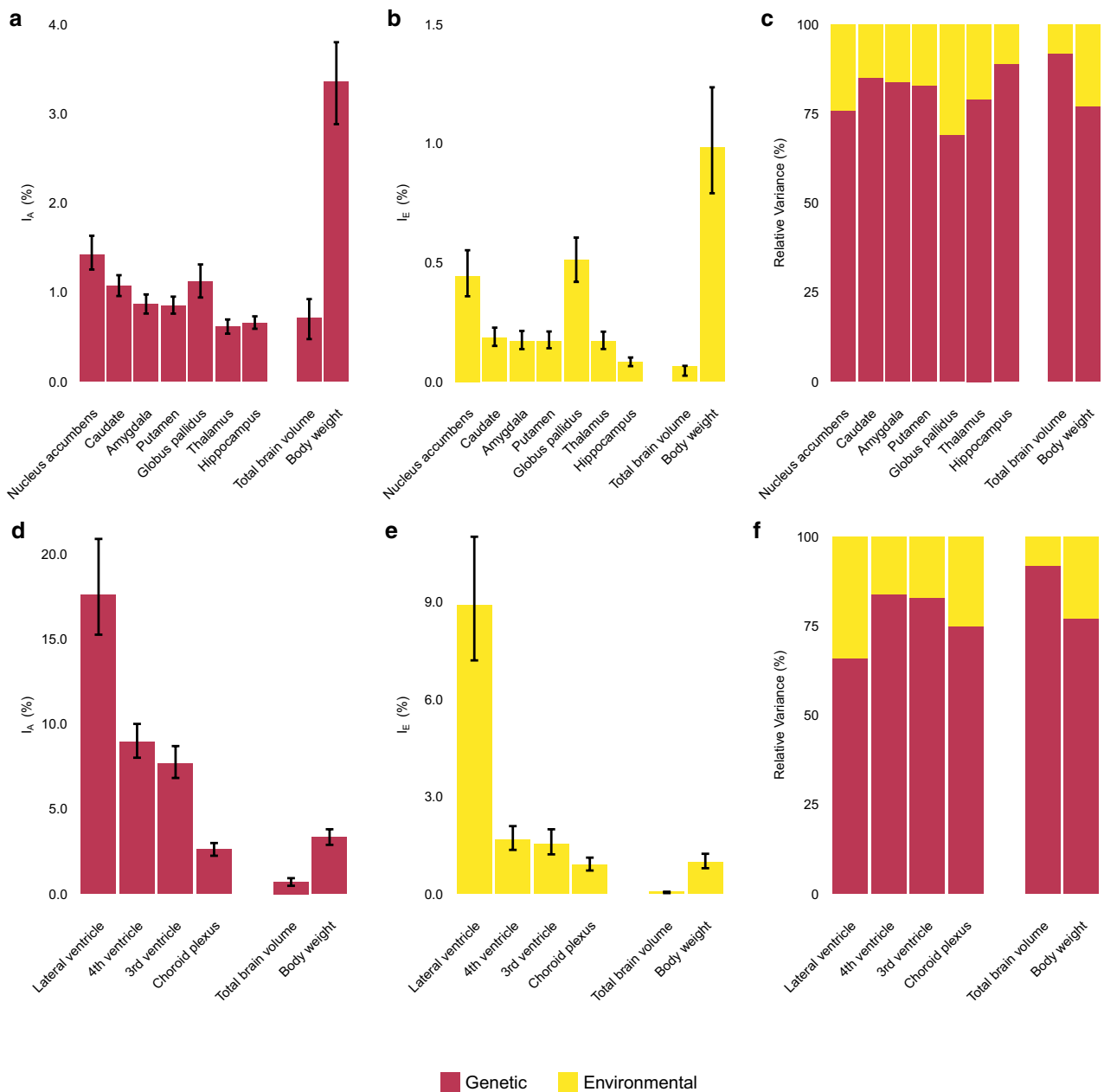


**Fig. 6** Absolute (mean-standardised) genetic (**a**, **d**) and environmental (**b**, **e**) variances (with 95% confidence intervals), as well as relative genetic and environmental variance components (**c**, **f**) for sub-

cortical (top row) and ventricular (bottom row) structures in the HCP data set. Estimates are presented in descending order of mean-standardised genetic variance in the QTIM data set (Fig. 3)

in a trait, and uses the phenotypic mean of the trait to scale variance components. Thus, estimates of mean-standardised variance are robust to other variance sources, and inform on the strength of factors which maintain or deplete variability in brain anatomy.

The most striking finding was the large mean-standardised variance for the ventricular system (particularly the lateral ventricles) compared to other brain structures, and that this substantial variance in ventricular volume was largely due to genetic factors. This is consistent with studies of

mean-standardised phenotypic variance (Lange et al. 1997; Allen et al. 2002), though estimates for lateral ventricle volume were substantially larger (40.32% and 47.75%, respectively) than those of the present examination (QTIM 19.06%, HCP 26.46%). This contrast is likely due to the small sample sizes ( $n = 115$  and 46, respectively) and superseded imaging methods of past studies. Here we showed that this high phenotypic variance is mainly due to genetic factors, with only a small amount of the variance attributed to the environment. The finding of large mean-standardised genetic

variance for ventricular volume (much larger than all other brain structures) is somewhat unexpected, as it is substantially higher than estimates for many morphological, life-history, and complex behavioural traits (Miller and Penke 2007; Garcia-Gonzalez et al. 2012; Houle 1992; Coltman et al. 2005). For instance, Hansen et al. (2011) report median mean-standardised genetic variance estimates of around 1% for weight-based size measures and life-history traits.

Why then would lateral ventricular volume show such large variation? Ventricular enlargement is often considered a marker of tissue atrophy in both normal ageing and disease (Apostolova et al. 2012; Nestor et al. 2008; Carmichael et al. 2007; Thompson et al. 2006), but estimates in the present study were of healthy adults. Previous studies have suggested the large mean-standardised phenotypic variance in the volume of the lateral ventricles reflects accumulated variability in surrounding structures (Lange et al. 1997); however, in the present study, we did not find large mean-standardised variance for surrounding subcortical structures, namely the hippocampus and caudate. The large variance found for some life-history traits (e.g., reproductive success, longevity) is typically explained by the composite nature of these traits, which integrate variation across the lifespan. Because of this, it is likely that a greater number of loci (and more mutations), more environmental variables, and the interactions between them, contribute to variation in life-history traits (Houle 1992; Hansen et al. 2011; Miller and Penke 2007). While not a life-history trait, the early embryonic development of the ventricular system (Lowery and Sive 2009), if influenced by many genetic and environmental factors, could explain the large mean-standardised variation in this structure.

The high mean-standardised variance (particularly genetic) for ventricular structures could also represent a lack of selection pressures (stabilising or directional) throughout evolution. All else being equal, brain structures that have been subject to strong selection should show less genetic variance than structures under weaker selection, as selection should deplete additive genetic variance (Barton and Keightley 2002). Hence, the larger mean-standardised genetic variance for ventricular structures might suggest a lack of strong selection, whereas the small genetic variance found for limbic system structures such as the hippocampus and thalamus might imply that the size of these structures was under stronger selection across evolution. Indeed, the contribution of genetic variants to human hippocampal volume was shown to be significantly greater in evolutionarily conserved regions compared to other functional categories of the genome (Hibar et al. 2017). Small variation for structures could further be interpreted in regards to canalisation: a narrowing of variation to increase robustness to genetic (and environmental) perturbations (Waddington 1942). From this perspective, stabilising selection may have resulted in

brain structures that are crucial to physiological and/or cognitive function evolving to a robust optimum. However, the all-else-is-equal assumption is paramount to these inferences. That is, for differences in genetic variance to reveal historical associations with selection, genetic architecture and other contributing factors should be comparable across brain structures, and our knowledge is limited in this respect. Conversely it is possible that high morphological variability does not imply a lack of function or selection pressures (as demonstrated by Kelly et al. (2018) in an examination of male and female nipple size).

It is important to also consider the role of ontogenetic (developmental) constraints when comparing variation between traits. For instance, the smaller mean-standardised genetic variance for cortical and subcortical brain structures ( $I_A$  range 0.52–2.01%) compared to body weight ( $I_A = 2.85\%$ ) might correspond to the stronger physical constraints over brain structure (which is constrained by the skull, dura matter, and subarachnoid space) compared to body weight (which can vary more freely). Interestingly, the larger variation in body weight is likely not entirely due to freely varying composition factors such as muscle, fat, and organ mass, as estimates of mean-standardised phenotypic variance for human skeletal weight [ $I_P$  range 1.97–4.39%, calculated from data reviewed by Wagner and Heyward (2000)] fall between the estimates for mean-standardised phenotypic variance in cortical/subcortical structures ( $I_P$  range 0.63–3.31%) and body weight ( $I_P = 3.76\%$ ) in the present study. Furthermore, the physical constraints imposed by the limited space available within the cranium likely impacts the variation of individual brain structures. As the ventricular system arises within the cavities of the primary brain vesicles (Lowery and Sive 2009; Carpenter 2016; Fujii et al. 2016), it begins to develop before subcortical and cortical structures. As a consequence, it may be under less strict physical constraints and vary more freely than later developing structures.

Measures of mean-standardised variance may shed light on the findings of past studies. ENIGMA, a worldwide consortium of brain imaging scientists, has conducted meta-analyses of case-control cohorts for a number of diseases, including major depressive disorder (Schmaal et al. 2016, 2017), schizophrenia (van Erp et al. 2016), bipolar disorder (Hibar et al. 2016) and attention deficit hyperactivity disorder (Hoogman et al. 2017). Of the subcortical structures examined so far in these analyses, the hippocampus is the only structure to show a statistically significant difference in the mean volume between patients and matched controls across all disorders (Thompson et al. 2017), and is the only subcortical structure to show a difference for major depressive disorder (Schmaal et al. 2016). This is noteworthy in the context of the present results, because mean-standardised phenotypic variance estimates for the hippocampus were the

lowest of the subcortical structures examined in the QTIM and HCP data sets. Therefore, the common finding of mean differences in hippocampal volume in all these analyses could reflect in part, the increased statistical power granted by the small variation present in (normal) hippocampal volume, which makes group differences easier to detect. The effect of normal variation and the sample size required to detect group differences should not be underestimated, especially as the high-price of in vivo imaging studies often prohibit large sample sizes. We suggest that future studies could carefully consider their research design and focus on structures with minimal phenotypic variance to maximise their statistical power.

The substantial mean-standardised environmental variance found for several structures should not be disregarded. Though differences in measures of mean-standardised environmental variance might be due to a range of factors (e.g., complexity of the phenotype, developmental constraint, interaction with external environment, measurement error), they are of great importance as they demonstrate that the unusually low relative genetic variance (i.e., heritability) of several brain structures (e.g., caudal anterior cingulate  $h^2 = 42%$  entorhinal cortex  $h^2 = 44%$ ) were not a result of unusually low levels of mean-standardised additive genetic variance in these structures (e.g., caudal anterior cingulate  $I_A = 1.15%$ ,  $I_E = 1.59%$ ; entorhinal cortex  $I_A = 1.42%$ ,  $I_E = 1.77%$ ).

Mean-standardised variance estimates differed between QTIM and HCP, though the patterns of variation were similar. The most prominent difference between the samples was in the lateral ventricles (QTIM  $I_A = 12.28%$ , HCP  $I_A = 17.58%$ ). Interestingly, even if participants are excluded based on their ventricle-to-brain ratio (outliers at  $\pm 3.29$  SD excluded), mean-standardised variance estimates for the lateral ventricles remain larger in the HCP data set ( $I_A = 14.40%$ ) compared to the QTIM data set ( $I_A = 11.99%$ ). These differences in genetic variance could reflect sampling error due to the small sample size of twins used to distinguish genetic from environmental variance. However, estimates of mean-standardised phenotypic variance (which are more stable than genetic/environmental) for the lateral ventricles also differed between the data sets (HCP  $I_p = 26.46%$ , QTIM  $I_p = 19.06%$ ), suggesting that sampling error is unlikely to be the main cause of this difference. As QTIM is a predominantly Caucasian sample, it is possible that differences in variance component estimates reflect the more diverse ethnic and racial composition of the HCP sample, which approximates that of the U.S. population (Van Essen et al. 2013). Furthermore, the HCP data set is more varied than the QTIM data set in terms of participants' drinking and recreational drug use history (Van Essen et al. 2013). Differences in measurement error (reflected in test–retest reliability ICCs) could additionally contribute to differences

in structure variability between the data sets (e.g., temporal pole).

In the present study, we found no association between mean-standardised and relative measures of genetic variance for brain structure volumes. Though this was expected based on studies of other biological and life-history traits (Houle 1992; Hansen et al. 2011), it was important to empirically demonstrate this for human brain morphology. The lack of a strong association between absolute and relative genetic variance is significant, as it indicates that new insights into brain development could be gained from changing the way in which the variance components of brain structure are considered. For example, investigating amounts of mean-standardised variance (genetic/environmental) in brain structure for healthy controls and patients could reflect differences in the histogenetic processes underlying brain development between these groups. While further research is required to understand the implications of differences in mean-standardised absolute variance amounts, their usefulness may lie in elucidating patterns of genetic variance in the brain not visible through heritability estimates.

One limitation of mean-standardised absolute variance measures is that only traits on ratio or log-interval scale produce meaningful estimates (Hansen et al. 2011; Houle 1992), meaning that many human traits (e.g., intelligence) are unsuitable for mean-standardised measures. This limitation could be circumvented by future studies examining individual task scores (e.g., number of correct responses) rather than composite, factors scores. Curiously this has been examined in chimpanzees (e.g., spatial memory,  $I_A = 20.68%$ ) (Woodley Of Menie et al. 2015), but not in humans. Future studies could also use the multivariate nature of morphological brain measures (Renteria et al. 2014; Wen et al. 2016; Eyer et al. 2011) to produce new, multidimensional phenotypes, which will likely advance our understanding of structural variation in the brain beyond the univariate analyses of the present study.

This was the first comparison in humans of mean scaled measures of absolute variance (genetic and environmental) across brain structure volumes. We uncovered significant and, in some cases, striking variation in variances across different regions. This variation did not follow any obvious patterns, precluding straightforward explanations. These findings open important new lines of enquiry: namely, understanding the bases of these variance patterns, and their implications regarding the genetic architecture, evolution, and development of the human brain.

**Acknowledgements** We are forever grateful to the twins and siblings for their willingness to participate in our studies. We thank Marlene Grace and Ann Eldridge for participant recruitment; Kerrie McAloney for study co-ordination; Kori Johnson, Aaron Quiggle, Natalie Garden, Matthew Meredith, Peter Hobden, Kate Borg, Aiman Al Najjar and Anita Burns for data acquisition; David Butler and Daniel Park for IT

support. We additionally thank the two anonymous reviewers whose comments and suggestions helped improve this manuscript.

**Funding** The QTIM study was supported by the National Institute of Child Health and Human Development (R01 HD050735), and the National Health and Medical Research Council (NHMRC 486682, 1009064), Australia. Lachlan Strike was supported by an Australian Postgraduate Award (APA) scholarship and a Queensland Brain Institute (QBI) top-up scholarship. Data were provided [in part] by the Human Connectome Project, WU-Minn Consortium (Principal Investigators: David Van Essen and Kamil Ugurbil; 1U54MH091657) funded by the 16 NIH Institutes and Centers that support the NIH Blueprint for Neuroscience Research; and by the McDonnell Center for Systems Neuroscience at Washington University.

## Compliance with ethical standards

**Conflict of interest** The authors declare that they have no conflict of interest.

**Ethical approval** All procedures performed in studies involving human participants were in accordance with the ethical standards of the institutional and/or national research committee and with the 1964 Helsinki declaration and its later amendments or comparable ethical standards.

**Research involving human participants and/or animals** This article does not contain any studies with animals performed by any of the authors.

**Informed consent** Informed consent was obtained from all individual participants included in the study.

## References

- Allen JS, Damasio H, Grabowski TJ (2002) Normal neuroanatomical variation in the human brain: an MRI-volumetric study. *Am J Phys Anthropol* 118(4):341–358. <https://doi.org/10.1002/ajpa.10092>
- Apostolova LG, Green AE, Babakchianian S, Hwang KS, Chou YY, Toga AW, Thompson PM (2012) Hippocampal atrophy and ventricular enlargement in normal aging, mild cognitive impairment (MCI), and Alzheimer Disease. *Alzheimer Dis Assoc Disord* 26(1):17–27. <https://doi.org/10.1097/WAD.0b013e3182163b62>
- Barton NH, Keightley PD (2002) Understanding quantitative genetic variation. *Nat Rev Genet* 3(1):11–21. <https://doi.org/10.1038/nrg700>
- Blokland GA, McMahon KL, Thompson PM, Hickie IB, Martin NG, de Zubicaray GI, Wright MJ (2014) Genetic effects on the cerebellar role in working memory: same brain, different genes? *Neuroimage* 86(C):392–403. <https://doi.org/10.1016/j.neuroimage.2013.10.006>
- Carmichael OT, Kuller LH, Lopez OL, Thompson PM, Dutton RA, Lu A, Lee SE, Lee JY, Aizenstein HJ, Meltzer CC, Liu Y, Toga AW, Becker JT (2007) Ventricular volume and dementia progression in the Cardiovascular Health Study. *Neurobiol Aging* 28(3):389–397. <https://doi.org/10.1016/j.neurobiolaging.2006.01.006>
- Carpenter EM (2016) Development of brain ventricles and choroid plexus. In: Chen TC (ed) *The choroid plexus and cerebrospinal fluid*. Academic Press, San Diego, pp 15–27. <https://doi.org/10.1016/b978-0-12-801740-1.00002-0>
- Charlesworth B (1984) The evolutionary genetics of life histories. In: Shorrocks B (ed) *Evolutionary ecology*. Blackwell Publishers, Oxford
- Charlesworth B (1987) The heritability of fitness. In: Bradbury JW, Andersson MB (eds) *Sexual selection: testing the alternatives*. Wiley, New York, pp 21–40
- Chiang MC, McMahon KL, de Zubicaray GI, Martin NG, Hickie I, Toga AW, Wright MJ, Thompson PM (2011) Genetics of white matter development: a DTI study of 705 twins and their siblings aged 12–29. *Neuroimage* 54(3):2308–2317. <https://doi.org/10.1016/j.neuroimage.2010.10.015>
- Coltman DW, O’Donoghue P, Hogg JT, Festa-Bianchet M (2005) Selection and genetic (co)variance in bighorn sheep. *Evolution* 59(6):1372–1382. <https://doi.org/10.1111/j.0014-3820.2005.tb01786.x>
- Core Team R (2019) R: a language and environment for statistical computing. R Foundation for Statistical Computing, Vienna
- de Leeuw J (1992) Introduction to Akaike (1973) information theory and an extension of the maximum likelihood principle. In: Kotz S, Johnson NL (eds) *Breakthroughs in statistics*. Springer series in statistics. Springer, New York, pp 599–609. [https://doi.org/10.1007/978-1-4612-0919-5\\_37](https://doi.org/10.1007/978-1-4612-0919-5_37)
- de Zubicaray GI, Chiang MC, McMahon KL, Shattuck DW, Toga AW, Martin NG, Wright MJ, Thompson PM (2008) Meeting the challenges of neuroimaging genetics. *Brain Imaging Behav* 2(4):258–263. <https://doi.org/10.1007/s11682-008-9029-0>
- Desikan RS, Segonne F, Fischl B, Quinn BT, Dickerson BC, Blacker D, Buckner RL, Dale AM, Maguire RP, Hyman BT, Albert MS, Killiany RJ (2006) An automated labeling system for subdividing the human cerebral cortex on MRI scans into gyral based regions of interest. *Neuroimage* 31(3):968–980. <https://doi.org/10.1016/j.neuroimage.2006.01.021>
- Eyler LT, Prom-Wormley E, Fennema-Notestine C, Panizzon MS, Neale MC, Jernigan TL, Fischl B, Franz CE, Lyons MJ, Stevens A, Pacheco J, Perry ME, Schmitt JE, Spitzer NC, Seidman LJ, Thermonos HW, Tsuang MT, Dale AM, Kremen WS (2011) Genetic patterns of correlation among subcortical volumes in humans: results from a magnetic resonance imaging twin study. *Hum Brain Mapp* 32(4):641–653. <https://doi.org/10.1002/hbm.21054>
- Fischl B (2012) FreeSurfer. *Neuroimage* 62(2):774–781. <https://doi.org/10.1016/j.neuroimage.2012.01.021>
- Fujii T, Youssefzadeh J, Novel M, Neman J (2016) Introduction to the ventricular system and choroid plexus. In: Neman J, Chen TC (eds) *The choroid plexus and cerebrospinal fluid*, 1st edn. Academic Press, San Diego, pp 1–13. <https://doi.org/10.1016/b978-0-12-801740-1.00001-9>
- Garcia-Gonzalez F, Simmons LW, Tomkins JL, Kotiaho JS, Evans JP (2012) Comparing evolvabilities: common errors surrounding the calculation and use of coefficients of additive genetic variation. *Evolution* 66(8):2341–2349. <https://doi.org/10.1111/1/j.1558-5646.2011.01565.x>
- Glasser MF, Coalson TS, Robinson EC, Hacker CD, Harwell J, Yacoub E, Ugurbil K, Andersson J, Beckmann CF, Jenkinson M, Smith SM, Van Essen DC (2016) A multi-modal parcellation of human cerebral cortex. *Nature* 536(7615):171–178. <https://doi.org/10.1038/nature18933>
- Gu J, Kanai R (2014) What contributes to individual differences in brain structure? *Front Hum Neurosci* 8:262. <https://doi.org/10.3389/fnhum.2014.00262>
- Hansen TF, Pelabon C, Armbruster WS, Carlson ML (2003) Evolvability and genetic constraint in *Dalechampia* blossoms: components of variance and measures of evolvability. *J Evol Biol* 16(4):754–766
- Hansen TF, Pélabon C, Houle D (2011) Heritability is not evolvability. *Evol Biol* 38(3):258–277
- Hibar DP, Westlye LT, van Erp TG, Rasmussen J, Leonardo CD, Faskowitz J, Haukvik UK, Hartberg CB, Doan NT, Agartz I, Dale AM, Gruber O, Kramer B, Trost S, Liberg B, Abe C, Ekman CJ,

- Ingvar M, Landen M, Fears SC, Freimer NB, Bearden CE, Costa Rica/Colombia Consortium for Genetic Investigation of Bipolar E, Sprooten E, Glahn DC, Pearlson GD, Emsell L, Kenney J, Scanlon C, McDonald C, Cannon DM, Almeida J, Versace A, Caseras X, Lawrence NS, Phillips ML, Dima D, Delvecchio G, Frangou S, Satterthwaite TD, Wolf D, Houenou J, Henry C, Malt UF, Boen E, Elvsashagen T, Young AH, Lloyd AJ, Goodwin GM, Mackay CE, Bourne C, Bilderbeck A, Abramovic L, Boks MP, van Haren NE, Ophoff RA, Kahn RS, Bauer M, Pfenning A, Alda M, Hajek T, Mwangi B, Soares JC, Nickson T, Dimitrova R, Sussmann JE, Hagenaars S, Whalley HC, McIntosh AM, Thompson PM, Andreassen OA (2016) Subcortical volumetric abnormalities in bipolar disorder. *Mol Psychiatry* 21(12):1710–1716. <https://doi.org/10.1038/mp.2015.227>
- Hibar DP, Adams HHH, Jahanshad N, Chauhan G, Stein JL, Hofer E, Renteria ME, Bis JC, Arias-Vasquez A, Ikram MK, Desrivieres S, Vernooij MW, Abramovic L, Alhusaini S, Amin N, Andersson M, Arfanakis K, Aribisala BS, Armstrong NJ, Athanasios L, Axelsson T, Beecham AH, Beiser A, Bernard M, Blanton SH, Bohlken MM, Boks MP, Bralten J, Brickman AM, Carmichael O, Chakravarty MM, Chen Q, Ching CRK, Chouraki V, Cuellar-Partida G, Crivello F, Den Braber A, Doan NT, Ehrlich S, Giddaluru S, Goldman AL, Gottesman RF, Grimm O, Griswold ME, Guadalupe T, Gutman BA, Hass J, Haukvik UK, Hoehn D, Holmes AJ, Hoogman M, Janowitz D, Jia T, Jorgensen KN, Karbalai N, Kasperaviciute D, Kim S, Klein M, Kraemer B, Lee PH, Liewald DCM, Lopez LM, Luciano M, Macare C, Marquand AF, Matarin M, Mather KA, Mattheisen M, McKay DR, Milanesechi Y, Munoz Maniega S, Nho K, Nugent AC, Nyquist P, Loohuis LMO, Oosterlaan J, Papmeyer M, Pirpamer L, Putz B, Ramasamy A, Richards JS, Risacher SL, Roiz-Santianez R, Rommelse N, Ropele S, Rose EJ, Royle NA, Rundek T, Samann PG, Saremi A, Satizabal CL, Schmaal L, Schork AJ, Shen L, Shin J, Shumskaya E, Smith AV, Sprooten E, Strike LT, Teumer A, Tordesillas-Gutierrez D, Toro R, Trabzuni D, Trompet S, Vaidya D, Van der Grond J, Van der Lee SJ, Van der Meer D, Van Donkelaar MMJ, Van Eijk KR, Van Erp TGM, Van Rooij D, Walton E, Westlye LT, Whelan CD, Windham BG, Winkler AM, Wittfeld K, Woldehawariat G, Wolf C, Wolfers T, Yanek LR, Yang J, Zijdenbos A, Zwiwers MP, Agartz I, Almasy L, Ames D, Amouyel P, Andreassen OA, Arepalli S, Assareh AA, Barral S, Bastin ME, Becker DM, Becker JT, Bennett DA, Blangero J, van Bokhoven H, Boomsma DI, Brodaty H, Brouwer RM, Brunner HG, Buckner RL, Buitelaar JK, Bulayeva KB, Cahn W, Calhoun VD, Cannon DM, Cavalleri GL, Cheng CY, Cichon S, Cookson MR, Corvin A, Crespo-Facorro B, Curran JE, Czisch M, Dale AM, Davies GE, De Craen AJM, De Geus EJC, De Jager PL, De Zubicaray GI, Deary IJ, Debette S, DeCarli C, Delanty N, Depondt C, DeStefano A, Dillman A, Djurovic S, Donohoe G, Drevets WC, Duggirala R, Dyer TD, Enzinger C, Erk S, Espeseth T, Fedko IO, Fernandez G, Ferrucci L, Fisher SE, Fleischman DA, Ford I, Fornage M, Foroud TM, Fox PT, Francks C, Fukunaga M, Gibbs JR, Glahn DC, Gollub RL, Goring HHH, Green RC, Gruber O, Gudnason V, Guelfi S, Haberg AK, Hansell NK, Hardy J, Hartman CA, Hashimoto R, Hegenscheid K, Heinz A, Le Hellard S, Hernandez DG, Heslenfeld DJ, Ho BC, Hoekstra PJ, Hoffmann W, Hofman A, Holsboer F, Homuth G, Hosten N, Hottenga JJ, Huettelman M, Hulshoff Pol HE, Ikeda M, Jack CR Jr, Jenkinson M, Johnson R, Jonsson EG, Jukema JW, Kahn RS, Kanai R, Kloszewska I, Knopman DS, Kochunov P, Kwok JB, Lawrie SM, Lemaître H, Liu X, Longo DL, Lopez OL, Lovestone S, Martinez O, Martinot JL, Mattay VS, McDonald C, McIntosh AM, McMahon FJ, McMahon KL, Mecocci P, Melle I, Meyer-Lindenberg A, Mohnke S, Montgomery GW, Morris DW, Mosley TH, Muhleisen TW, Muller-Myhsok B, Nalls MA, Nauck M, Nichols TE, Niessen WJ, Nothen MM, Nyberg L, Ohi K, Olvera RL, Ophoff RA, Pandolfo M, Paus T, Pausova Z, Penninx B, Pike GB, Potkin SG, Psaty BM, Reppermund S, Rietschel M, Roffman JL, Romanczuk-Seiferth N, Rotter JI, Ryten M, Sacco RL, Sachdev PS, Saykin AJ, Schmidt R, Schmidt H, Schofield PR, Sigurdson S, Simmons A, Singleton A, Sisodiya SM, Smith C, Smoller JW, Soininen H, Steen VM, Stott DJ, Sussmann JE, Thalamuthu A, Toga AW, Traynor BJ, Troncoso J, Tsolaki M, Tzourio C, Uitterlinden AG, Hernandez MCV, Van der Brug M, van der Lugt A, van der Wee NJA, Van Haren NEM, van't Ent D, Van Tol MJ, Vardarajan BN, Vellas B, Veltman DJ, Volzke H, Walter H, Wardlaw JM, Wassink TH, Weale ME, Weinberger DR, Weiner MW, Wen W, Westman E, White T, Wong TY, Wright CB, Zielke RH, Zonderman AB, Martin NG, Van Duijn CM, Wright MJ, Longstreth WT, Schumann G, Grabe HJ, Franke B, Launer LJ, Medland SE, Seshadri S, Thompson PM, Ikram MA (2017) Novel genetic loci associated with hippocampal volume. *Nat Commun* 8:13624. <https://doi.org/10.1038/ncomms13624>
- Hoogman M, Bralten J, Hibar DP, Mennes M, Zwiwers MP, Schwersen LSJ, van Hulzen KJE, Medland SE, Shumskaya E, Jahanshad N, Zeeuw P, Szekely E, Sudre G, Wolfers T, Onnink AMH, Dammers JT, Mostert JC, Vives-Gilabert Y, Kohls G, Oberwilling E, Seitz J, Schulte-Ruther M, Ambrosino S, Doyle AE, Hovik MF, Dramsdahl M, Tamm L, van Erp TGM, Dale A, Schork A, Conzelmann A, Zierhut K, Baur R, McCarthy H, Yoncheva YN, Cubillo A, Chantiluke K, Mehta MA, Paloyelis Y, Hohmann S, Baumeister S, Bramati I, Mattos P, Tovar-Moll F, Douglas P, Banaschewski T, Brandeis D, Kuntsi J, Asherson P, Rubia K, Kelly C, Martino AD, Milham MP, Castellanos FX, Frodl T, Zentis M, Lesch KP, Reif A, Pauli P, Jernigan TL, Haavik J, Plessen KJ, Lundervold AJ, Hugdahl K, Seidman LJ, Biederman J, Rommelse N, Heslenfeld DJ, Hartman CA, Hoekstra PJ, Oosterlaan J, Polier GV, Konrad K, Vilarroya O, Ramos-Quiroga JA, Soliva JC, Durston S, Buitelaar JK, Faraone SV, Shaw P, Thompson PM, Franke B (2017) Subcortical brain volume differences in participants with attention deficit hyperactivity disorder in children and adults: a cross-sectional mega-analysis. *Lancet Psychiatry* 4(4):310–319. [https://doi.org/10.1016/S2215-0366\(17\)30049-4](https://doi.org/10.1016/S2215-0366(17)30049-4)
- Houle D (1992) Comparing evolvability and variability of quantitative traits. *Genetics* 130(1):195–204
- Jansen AG, Mous SE, White T, Posthuma D, Polderman TJ (2015) What twin studies tell us about the heritability of brain development, morphology, and function: a review. *Neuropsychol Rev* 25(1):27–46. <https://doi.org/10.1007/s11065-015-9278-9>
- Joshi AA, Lepore N, Joshi SH, Lee AD, Barysheva M, Stein JL, McMahon KL, Johnson K, de Zubicaray GI, Martin NG, Wright MJ, Toga AW, Thompson PM (2011) The contribution of genes to cortical thickness and volume. *Neuroreport* 22(3):101–105. <https://doi.org/10.1097/WNR.0b013e3283424c84>
- Kelly AJ, Dubbs SL, Barlow FK, Zietsch BP (2018) Male and female nipples as a test case for the assumption that functional features vary less than nonfunctional byproducts. *Adapt Hum Behav Phys* 4(4):344–353. <https://doi.org/10.1007/s40750-018-0096-1>
- Kennedy DN, Lange N, Makris N, Bates J, Meyer J, Caviness VS Jr (1998) Gyri of the human neocortex: an MRI-based analysis of volume and variance. *Cereb Cortex (New York, NY: 1991)* 8(4):372–384. <https://doi.org/10.1093/cercor/8.4.372>
- Kremen WS, Prom-Wormley E, Panizzon MS, Eyer LT, Fischl B, Neale MC, Franz CE, Lyons MJ, Pacheco J, Perry ME, Stevens A, Schmitt JE, Grant MD, Seidman LJ, Thermenos HW, Tsuang MT, Eisen SA, Dale AM, Fennema-Notestine C (2010) Genetic and environmental influences on the size of specific brain regions in midlife: the VETSA MRI study. *Neuroimage* 49(2):1213–1223. <https://doi.org/10.1016/j.neuroimage.2009.09.043>
- Kremen WS, Panizzon MS, Neale MC, Fennema-Notestine C, Prom-Wormley E, Eyer LT, Stevens A, Franz CE, Lyons MJ, Grant MD, Jak AJ, Jernigan TL, Xian H, Fischl B, Thermenos HW, Seidman LJ, Tsuang MT, Dale AM (2012) Heritability of brain

- ventricle volume: converging evidence from inconsistent results. *Neurobiol Aging* 33(1):1–8. <https://doi.org/10.1016/j.neurobiolaging.2010.02.007>
- Lange N, Giedd JN, Castellanos FX, Vaituzis AC, Rapoport JL (1997) Variability of human brain structure size: ages 4–20 years. *Psychiatry Res* 74(1):1–12. [https://doi.org/10.1016/S0925-4927\(96\)03054-5](https://doi.org/10.1016/S0925-4927(96)03054-5)
- Lowery LA, Sive H (2009) Totally tubular: the mystery behind function and origin of the brain ventricular system. *Bioessays* 31(4):446–458. <https://doi.org/10.1002/bies.200800207>
- Miller GF, Penke L (2007) The evolution of human intelligence and the coefficient of additive genetic variance in human brain size. *Intelligence* 35(2):97–114. <https://doi.org/10.1016/j.intell.2006.08.008>
- Neale MC, Cardon LR (1992) Methodology for genetic studies of twins and families. Kluwer Academic Publishers, Dordrecht
- Neale MC, Hunter MD, Pritikin JN, Zahery M, Brick TR, Kirkpatrick RM, Estabrook R, Bates TC, Maes HH, Boker SM (2016) OpenMx 2.0: extended structural equation and statistical modeling. *Psychometrika* 81(2):535–549. <https://doi.org/10.1007/s11336-014-9435-8>
- Nestor SM, Rupsingh R, Borrie M, Smith M, Accomazzi V, Wells JL, Fogarty J, Bartha R, Alzheimer's Disease Neuroimaging I (2008) Ventricular enlargement as a possible measure of Alzheimer's disease progression validated using the Alzheimer's disease neuroimaging initiative database. *Brain* 131(Pt 9):2443–2454. <https://doi.org/10.1093/brain/awn146>
- Noreikiene K, Herczeg G, Gonda A, Balazs G, Husby A, Merila J (2015) Quantitative genetic analysis of brain size variation in sticklebacks: support for the mosaic model of brain evolution. *Proc Biol Sci*. <https://doi.org/10.1098/rspb.2015.1008>
- Posthuma D, Boomsma DI (2000) A note on the statistical power in extended twin designs. *Behav Genet* 30(2):147–158. <https://doi.org/10.1023/A:1001959306025>
- Renteria ME, Hansell NK, Strike LT, McMahon KL, de Zubicaray GI, Hickie IB, Thompson PM, Martin NG, Medland SE, Wright MJ (2014) Genetic architecture of subcortical brain regions: common and region-specific genetic contributions. *Genes Brain Behav* 13(8):821–830. <https://doi.org/10.1111/gbb.12177>
- Schmaal L, Veltman DJ, van Erp TG, Samann PG, Frodl T, Jahanshad N, Loehrer E, Tiemeier H, Hofman A, Niessen WJ, Vernooij MW, Ikram MA, Wittfeld K, Grabe HJ, Block A, Hegenscheid K, Volzke H, Hoehn D, Czisch M, Lagopoulos J, Hatton SN, Hickie IB, Goya-Maldonado R, Kramer B, Gruber O, Couvy-Duchesne B, Renteria ME, Strike LT, Mills NT, de Zubicaray GI, McMahon KL, Medland SE, Martin NG, Gillespie NA, Wright MJ, Hall GB, MacQueen GM, Frey EM, Carballo A, van Velzen LS, van Tol MJ, van der Wee NJ, Veer IM, Walter H, Schnell K, Schramm E, Normann C, Schoepf D, Konrad C, Zurowski B, Nickson T, McIntosh AM, Pappmeyer M, Whalley HC, Sussmann JE, Godlewska BR, Cowen PJ, Fischer FH, Rose M, Penninx BW, Thompson PM, Hibar DP (2016) Subcortical brain alterations in major depressive disorder: findings from the ENIGMA Major Depressive Disorder working group. *Mol Psychiatry* 21(6):806–812. <https://doi.org/10.1038/mp.2015.69>
- Schmaal L, Hibar DP, Samann PG, Hall GB, Baune BT, Jahanshad N, Cheung JW, van Erp TGM, Bos D, Ikram MA, Vernooij MW, Niessen WJ, Tiemeier H, Hofman A, Wittfeld K, Grabe HJ, Janowitz D, Bulow R, Selonke M, Volzke H, Grotegerd D, Dannlowski U, Arolt V, Opel N, Heindel W, Kugel H, Hoehn D, Czisch M, Couvy-Duchesne B, Renteria ME, Strike LT, Wright MJ, Mills NT, de Zubicaray GI, McMahon KL, Medland SE, Martin NG, Gillespie NA, Goya-Maldonado R, Gruber O, Kramer B, Hatton SN, Lagopoulos J, Hickie IB, Frodl T, Carballo A, Frey EM, van Velzen LS, Penninx B, van Tol MJ, van der Wee NJ, Davey CG, Harrison BJ, Mwangi B, Cao B, Soares JC, Veer IM, Walter H, Schoepf D, Zurowski B, Konrad C, Schramm E, Normann C, Schnell K, Sacchet MD, Gotlib IH, MacQueen GM, Godlewska BR, Nickson T, McIntosh AM, Pappmeyer M, Whalley HC, Hall J, Sussmann JE, Li M, Walter M, Aftanas L, Brack I, Bokhan NA, Thompson PM, Veltman DJ (2017) Cortical abnormalities in adults and adolescents with major depression based on brain scans from 20 cohorts worldwide in the ENIGMA Major Depressive Disorder Working Group. *Mol Psychiatry* 22(6):900–909. <https://doi.org/10.1038/mp.2016.60>
- Schmitt JE, Neale MC, Fassassi B, Perez J, Lenroot RK, Wells EM, Giedd JN (2014) The dynamic role of genetics on cortical patterning during childhood and adolescence. *Proc Natl Acad Sci USA* 111(18):6774–6779. <https://doi.org/10.1073/pnas.1311630111>
- Thompson PM, Dutton RA, Hayashi KM, Lu A, Lee SE, Lee JY, Lopez OL, Aizenstein HJ, Toga AW, Becker JT (2006) 3D mapping of ventricular and corpus callosum abnormalities in HIV/AIDS. *Neuroimage* 31(1):12–23. <https://doi.org/10.1016/j.neuroimage.2005.11.043>
- Thompson PM, Andreassen OA, Arias-Vasquez A, Bearden CE, Boedhoe PS, Brouwer RM, Buckner RL, Buitelaar JK, Bulayeva KB, Cannon DM, Cohen RA, Conrod PJ, Dale AM, Deary IJ, Dennis EL, de Reus MA, Desrivieres S, Dima D, Donohoe G, Fisher SE, Fouche JP, Francks C, Frangou S, Franke B, Ganjgahi H, Garavan H, Glahn DC, Grabe HJ, Guadalupe T, Gutman BA, Hashimoto R, Hibar DP, Holland D, Hoogman M, Pol HEH, Hosten N, Jahanshad N, Kelly S, Kochunov P, Kremen WS, Lee PH, Mackey S, Martin NG, Mazoyer B, McDonald C, Medland SE, Morey RA, Nichols TE, Paus T, Pausova Z, Schmaal L, Schumann G, Shen L, Sisodiya SM, Smit DJA, Smoller JW, Stein DJ, Stein JL, Toro R, Turner JA, van den Heuvel MP, van den Heuvel OL, van Erp TGM, van Rooij D, Veltman DJ, Walter H, Wang Y, Wardlaw JM, Whelan CD, Wright MJ, Ye J, Consortium E (2017) ENIGMA and the individual: Predicting factors that affect the brain in 35 countries worldwide. *Neuroimage* 145(Pt B):389–408. <https://doi.org/10.1016/j.neuroimage.2015.11.057>
- van Erp TG, Hibar DP, Rasmussen JM, Glahn DC, Pearlson GD, Andreassen OA, Agartz I, Westlye LT, Haukvik UK, Dale AM, Melle I, Hartberg CB, Gruber O, Kraemer B, Zilles D, Donohoe G, Kelly S, McDonald C, Morris DW, Cannon DM, Corvin A, Machielsen MW, Koenders L, de Haan L, Veltman DJ, Satterthwaite TD, Wolf DH, Gur RC, Gur RE, Potkin SG, Mathalon DH, Mueller BA, Preda A, Macciardi F, Ehrlich S, Walton E, Hass J, Calhoun VD, Bockholt HJ, Sponheim SR, Shoemaker JM, van Haren NE, Hulshoff Pol HE, Ophoff RA, Kahn RS, Roiz-Santianez R, Crespo-Facorro B, Wang L, Alpert KI, Jonsson EG, Dimitrova R, Bois C, Whalley HC, McIntosh AM, Lawrie SM, Hashimoto R, Thompson PM, Turner JA (2016) Subcortical brain volume abnormalities in 2028 individuals with schizophrenia and 2540 healthy controls via the ENIGMA consortium. *Mol Psychiatry* 21(4):547–553. <https://doi.org/10.1038/mp.2015.63>
- Van Essen DC, Ugurbil K, Auerbach E, Barch D, Behrens TE, Bucholz R, Chang A, Chen L, Corbetta M, Curtiss SW, Della Penna S, Feinberg D, Glasser MF, Harel N, Heath AC, Larson-Prior L, Marcus D, Michalareas G, Moeller S, Oostenveld R, Petersen SE, Prior F, Schlaggar BL, Smith SM, Snyder AZ, Xu J, Yacoub E, Consortium WU-MH (2012) The Human Connectome Project: a data acquisition perspective. *Neuroimage* 62(4):2222–2231. <https://doi.org/10.1016/j.neuroimage.2012.02.018>
- Van Essen DC, Smith SM, Barch DM, Behrens TE, Yacoub E, Ugurbil K, Consortium WU-MH (2013) The WU-Minn Human Connectome Project: an overview. *Neuroimage* 80:62–79. <https://doi.org/10.1016/j.neuroimage.2013.05.041>
- Waddington CH (1942) Canalization of development and the inheritance of acquired characters. *Nature* 150(3811):563–565. <https://doi.org/10.1038/150563a0>

- Wagner DR, Heyward VH (2000) Measures of body composition in blacks and whites: a comparative review. *Am J Clin Nutr* 71(6):1392–1402. <https://doi.org/10.1093/ajcn/71.6.1392>
- Wen W, Thalamuthu A, Mather KA, Zhu W, Jiang J, de Micheaux PL, Wright MJ, Ames D, Sachdev PS (2016) Distinct genetic influences on cortical and subcortical brain structures. *Sci Rep* 6:32760. <https://doi.org/10.1038/srep32760>
- Whelan CD, Hibar DP, van Velzen LS, Zannas AS, Carrillo-Roa T, McMahon K, Prasad G, Kelly S, Faskowitz J, deZubiracay G, Iglesias JE, van Erp TGM, Frodl T, Martin NG, Wright MJ, Jahanshad N, Schmaal L, Samann PG, Thompson PM, Alzheimer's Disease Neuroimaging I (2016) Heritability and reliability of automatically segmented human hippocampal formation subregions. *Neuroimage* 128:125–137. <https://doi.org/10.1016/j.neuroimage.2015.12.039>
- Winkler AM, Kochunov P, Blangero J, Almasy L, Zilles K, Fox PT, Duggirala R, Glahn DC (2010) Cortical thickness or grey matter volume? The importance of selecting the phenotype for imaging genetics studies. *Neuroimage* 53(3):1135–1146. <https://doi.org/10.1016/j.neuroimage.2009.12.028>
- Woodley Of Menie MA, Fernandes HBF, Hopkins WD (2015) The more g-loaded, the more heritable, evolvable, and phenotypically variable: homology with humans in chimpanzee cognitive abilities. *Intelligence* 50:159–163. <https://doi.org/10.1016/j.intel.2015.04.002>

**Publisher's Note** Springer Nature remains neutral with regard to jurisdictional claims in published maps and institutional affiliations.